ON NEED FOR TOPOLOGY AWARENESS OF GENERATIVE MODELS

Uyeong Jang

Department of Computer Sciences University of Wisconsin–Madison Madison, WI 53706, USA wjang@cs.wisc.edu

Somesh Jha

Department of Computer Sciences University of Wisconsin–Madison Madison, WI 53706, USA jha@cs.wisc.edu

Susmit Jha

Computer Scinece Laboratory SRI International Menlo Park, CA 94025, USA susmit.jha@sri.com

ABSTRACT

Manifold assumption in learning states that: the data lie approximately on a manifold of much lower dimension than the input space. Generative models learn to generate data according to the underlying data distribution. Generative models are used in various tasks, such as data augmentation and generating variation of images. This paper addresses the following question: do generative models need to be aware of the topology of the underlying data manifold in which the data lie? This paper suggests that the answer is yes and demonstrates that these can have ramifications on security-critical applications, such as generative-model based defenses for adversarial examples. We provide theoretical and experimental results to support our claims.

1 Introduction

In several domains natural data lies in a low-dimensional manifold (henceforth referred to as the manifold assumptions) Zhu & Goldberg (2009). Generative models attempt to learn to generate data according to the underlying data distribution (the input to a generative model is usually random noise from a known distribution, such as Gaussian or uniform). Generative models are very important in various Machine Learning (ML) tasks, such as data augmentation and generating variations of images and videos. There are various types of generative models in the literature, such as VAE Kingma & Welling (2013), GAN Goodfellow et al. (2014a) and reversible generative models, e.g. Real NVP Dinh et al. (2016).

This paper addresses the following question: do generative models need to aware of the topology of the underlying data manifold? This paper suggests that the answer is **yes**. Perhaps this is not as important in applications, such as generating variations of images. However, ignoring the topology of the manifold corresponding to the underlying data can have ramifications in security-critical applications. For example, there have been defenses proposed in the literature that use generative models (essentially these techniques "pull back a data point back into the manifold before prediction using the generative model) Ilyas et al. (2017)Samangouei et al. (2018). Therefore, if the generative model does not capture the topology of the underlying manifold, it can adversely affect these defenses. In these cases the underlying generative model is being used as an approximation of the underlying manifold.

Next we summarize our main result. Let $G: Z \to X$ be a generative model with $Z = X = \mathbb{R}^n$ and \mathcal{D}_Z is a distribution over \mathbb{R}^n . Distribution \mathcal{D}_Z and the generative model induce a distribution $\mathcal{D}_{G(Z)}$ over \mathbb{R}^n (i.e. the distribution of the random variable G(z) where $z \sim \mathcal{D}_Z$). Let \mathcal{D}_X be the data generating distribution. Moreover, let \mathcal{D}_X be distribution generated by n_X manifolds (distributions

generated by manifolds is formalized in section 3) and \mathcal{D}_Z be generated by n_Z manifolds. Our main result is that if $n_Z < n_X$, then there is a topological mismatch between \mathcal{D}_X and $\mathcal{D}_{G(Z)}$. This indicates that the generative model should be given an advice string about the number of underlying manifolds. Our experimental results first confirm our theoretical results, then verify the usefulness of topology-aware model in the applications of generative models. Specifically, we visually confirm the main theorem, present the potential drawback of traditional topology-ignorant models in security-related application, and suggest the solution by training the generative model with a proper knowledge about the distribution topology.

We begin with a brief description of related works in section 2, Section 3 will provide the mathematical background of this project. Then, in section 4, the main theoretical contribution will be provided. Section 5 will demonstrate the experimental verification of theorems and its application.

2 RELATED WORK

2.1 Generative models

The field of generating natural samples has become one of the most successful application of *deep neural network (DNN)*. As a method of sampling high dimensional data, generative models find applications in various fields in applied math and engineering, e.g. image processing, reinforcement learning, etc.. Learning data generating distribution with neural networks includes well-known examples of *Variational Autoencoder (VAE)* Kingma & Welling (2013) and variations of *Generative Adversarial Network (GAN)* Goodfellow et al. (2014a)Radford et al. (2015)Zhao et al. (2016).

In this project, we mostly discuss generative models learning how to map latent variables into the generated samples. The forementioned VAE and GAN satisfy this property as both learn how to map latent vectors into generated samples. VAE is an example of variational Bayesian approach, which approximates posterior distribution over latent vectors (given training samples) by a simpler variational distribution. As other variational Bayesian methods do, VAE tries to minimize the KL divergence between the posterior distribution and the variational distribution, which is acheived by minimizing the reconstruction error of the auto-encoder. GAN is another types of approach to learn mapping latent vectors to plausible samples. Unlike other other approaches, GAN learns the target distribution by training two networks – generator and discriminator – simultaneously. To explain, the training of GAN can be viewed as playing two-player minimax game between the generator network and the discriminator network.

In addition to generating plausible samples, some class of generative models constructs bijective relation between latent vector and generated samples, so that the probability density of the generated sample can be estimated. Due to its bijective nature, such class of generative models is called to be *reversible*, and contains seminal examples of *normailizing flow* Rezende & Mohamed (2015), *Masked Autoregressive Flow (MAF)* Papamakarios et al. (2017), *Real NVP* Dinh et al. (2016), and *Glow* Kingma & Dhariwal (2018).

2.2 APPLICATIONS OF GENERATIVE MODELS IN ADVERSARIAL MACHINE LEARNING

While DNN also facilitated the recent achievements of classifying data, the DNN based classifier has been shown to be vulnerable to adversarial attacks Goodfellow et al. (2014b)Szegedy et al. (2013)Papernot et al. (2016)Moosavi-Dezfooli et al. (2016)Madry et al. (2017). Several hypothesis try explaining such vulnerability Goodfellow et al. (2014b)Szegedy et al. (2013)Tanay & Griffin (2016)Feinman et al. (2017), and one of such explanation is that the adversarial examples lie far away from the data manifold. This idea leads to defense approaches making use of the geometry restored from the dataset – by projecting the given input to the nearest point in the data manifold.

To restore a low dimensional shape from a given dataset, generative model can be exploited. The main idea is to approximate the data generating distribution with a generative model, to facilitate searching over data manifold by searching over the space of latent vectors. The term *invert and classify (INC)* was coined to describe this type of defense Ilyas et al. (2017), and different types of generative models were tried to purify adversarial examples Song et al. (2017) Ilyas et al. (2017) Samangouei et al. (2018). Usually, the projection is done by search the latent vector that minimizes the geometric distance Ilyas et al. (2017) Samangouei et al. (2018). On the other hands, if the density estimation is available, searching for the latent vectors maximizing the density also works. For

example, PixelDefend Song et al. (2017) makes use of *PixelCNN* Oord et al. (2016) for density estimation procedure. However, despite of the promising theoretical background, it turned out that all of those method are still vulnerable Athalye et al. (2018) Ilyas et al. (2017).

While generative model can be a useful method to approximate the shape of the dataset, it is not the only way to make use of the local geometry of the shape. For example, recent approach Dubey et al. (2019) makes use of the classifications over a set of nearlest neighbors, then use the weighted average as the classification of the projected point.

3 BACKGROUND

We will formally describe data generation, based on the well-known manifold assumption; data tends to be distributed along a manifold whose dimension is lower than the underlying space. In our model of data generation, we provide a formal definitnion of *data generating manifold* M on which the data generating distribution lies, so that M conforms to the manifold assumption.

3.1 REQUIREMENTS

Real world data tends to be noisy, so they does not easily correspond to an underlying manifold. We first focus on an ideal case that data is generated solely from the manifold M without noise.

In the setting of classification with l labels, we consider submanifolds M_1,\ldots,M_l that correspond to the generation of data in each class $i\in\{1,\ldots,l\}$, respectively. We assume that any pair of those submanifolds are disjoint, i.e. $M_i\cap M_j=\emptyset$ for any $i\neq j$, whereas the resulting data distribution may contain ambiguities that can be classified into any of i and j. We set the data generating manifold M for all data as the union of submanifolds, $M=M_1\cup\ldots\cup M_l$.

In this section, we describe computing probabilities over M when it is a Riemannian manifold equipped with a Riemannian metric g (See Appendix A.2 for the definitnion). We discuss two essential components: (a) a density function p, and (b) a measure dM over the manifold M. We expect p and dM to satisfy the followings.

- (R1) For any measurable subset $A \subset M$, i.e. $\Pr[\mathbf{x} \in A] = \int_{\mathbf{x} \in A} p(\mathbf{x}) dM(\mathbf{x})$.
- (**R2**) p is zero everywhere out of M, i.e. $supp(p) = \{ \mathbf{x} \in \mathbb{R}^n \mid p(\mathbf{x}) > 0 \} \subseteq M$
- (R3) For any (\mathbf{x}, y) , \mathbf{x} is sampled from M_i if and only if y = i, i.e. $\Pr[\mathbf{x} \in M_i] = \Pr[y = i]$

When equipped with such probability density function p, we call M as a data generating manifold.

In reality, data generation is affected by noise, so not all data lie on the data generating manifold. Therefore, we incorporate the noise as an artifact of data generation, and extend the density on M to the density on entire \mathbb{R}^n by assigning local noise densities on M.

To elaborate, we think of a procedure that (1) samples a point \mathbf{x}_o from M first, (2) add a noise vector \mathbf{n} to get an observed point $\hat{\mathbf{x}} = \mathbf{x}_o + \mathbf{n}$. Here, the noise \mathbf{n} is a random vector sampled from a local probability distribution whose *noise density function* is $\nu_{\mathbf{x}_o}$. From now on, p_M denotes the extended density, with respect to M, in \mathbb{R}^n . For the extended density p_M , we require the following.

(R4) The translated noise density function, $\nu_{\mathbf{x}}(\hat{\mathbf{x}} - \mathbf{x})$, is the density of noise $\mathbf{n} = \hat{\mathbf{x}} - \mathbf{x}$ being chosen for a given \mathbf{x} , so it should be equal to the conditional density when $\mathbf{x}_o = \mathbf{x}$.

$$\nu_{\mathbf{x}}(\hat{\mathbf{x}} - \mathbf{x}) = \nu_{\mathbf{x}}(\mathbf{n}_{\mathbf{x}}) = p_M(\hat{\mathbf{x}}|\mathbf{x}_o = \mathbf{x})$$

3.2 Density from a data generating manifold

Probability over a Riemannian manifold Now we describe computing a probability of x being generated from a measurable subset A in a Riemannian manifold M.

We assume a k-dimensional manifold M to be equipped with a Riemannian metric g, a family of inner products $g_{\mathbf{x}}$ on tangent spaces $T_{\mathbf{x}}M$. In this case, g induces the volume measure dM for integration over M. If M is parametrized by $\mathbf{x} = X(\mathbf{u})$ for $\mathbf{u} \in D \subseteq \mathbb{R}^k$, the integration of a measurable density function p on M is as follows.

$$\int_{\mathbf{x} \in M} p(\mathbf{x}) dM(\mathbf{x}) = \int_{\mathbf{u} \in D} p(X(\mathbf{u})) \sqrt{\left| \det[g_{X(\mathbf{u})}] \right|} d\mathbf{u}$$
 (1)

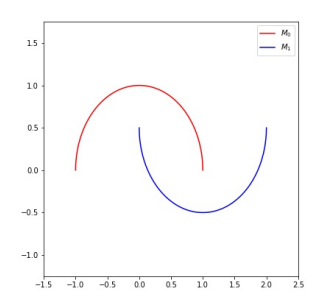
where $[g_{X(\mathbf{u})}]$ is the $k \times k$ matrix representation of the inner product $g_{X(\mathbf{u})}$ at $X(\mathbf{u}) \in M$.

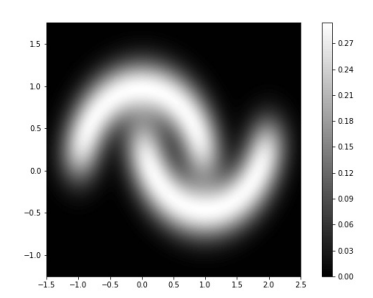
In the following section, a concrete example of this computation will be provided.

Computing density p over a Riemannian manifold M This section presents example computations of the probability computations from the Section 3.2 and 3.3 As a concrete example of computing density over a manifold, we use the following simple manifolds, so called *two-moons* in \mathbb{R}^2 .

$$\begin{split} M_0 &= \left\{ (x_1, x_2) \middle| \begin{array}{l} x_1 = \cos \theta \\ x_2 = \sin \theta \end{array} \right. \text{ for } \theta \in [0, \pi] \right\} \\ M_1 &= \left\{ (x_1, x_2) \middle| \begin{array}{l} x_1 = 1 - \cos \theta \\ x_2 = 1 - \sin \theta + \frac{1}{2} \end{array} \right. \text{ for } \theta \in [0, \pi] \right\} \end{split}$$

We take $M=M_0\cup M_1$ as our example manifold. Figure 1a shows the manifold of two-moons dataset plotted in different colors: M_0 in red and M_1 in blue.





- (a) Plot of the two-moons manifold in \mathbb{R}^2
- (b) Extended density function over \mathbb{R}^2 from the two-moons dataset

Figure 1: Density extension example from two-moons manifold.

First recall the following equation (equation (1) from the Section 3.2).

$$\int_{\mathbf{x}\in M} p(\mathbf{x}) dM(\mathbf{x}) = \int_{\mathbf{u}\in D} p(X(\mathbf{u})) \sqrt{\left|\det[g_{X(\mathbf{u})}]\right|} d\,\mathbf{u}$$

where $[g_{X(\mathbf{u})}]$ is the $k \times k$ matrix representation of the inner product $g_{X(\mathbf{u})}$ at $X(\mathbf{u}) \in M$.

Especially, when a manifold in \mathbb{R}^n is of dimension 1, i.e. parametrized curve $\gamma:[a,b]\to\mathbb{R}^n$, the integration (1) can be written in simpler way.

$$\int_{\mathbf{x}\in M} p(\mathbf{x})dM(\mathbf{x}) = \int_{t=a}^{b} p(\gamma(t)) \|\gamma'(t)\| dt$$
 (2)

where $\gamma'(t)$ is the *n*-dimensional velosity vector at $t \in [a, b]$.

Let p be a probability density function defined on M. As M is composed of two disjoint submanifolds M_0 and M_1 , we consider conditional densities p_0, p_1 as follows.

$$p_0(\mathbf{x}) = p(\mathbf{x} \mid \mathbf{x} \in M_0) = \frac{p|_{M_0}(\mathbf{x})}{\Pr[\mathbf{x} \in M_0]}$$

$$p_1(\mathbf{x}) = p(\mathbf{x} \mid \mathbf{x} \in M_1) = \frac{p|_{M_1}(\mathbf{x})}{\Pr[\mathbf{x} \in M_1]}$$
(3)

Here, $p|_{M_0}$ and $p|_{M_1}$ are the density function p with its domain restricted to M_0 and M_1 , respectively. By our definition of data generating manifolds, $\Pr[\mathbf{x} \in M_i]$ corresponds to the probability of data generation for class i, i.e. $\Pr[y=i]$. For a concrete example of such density, uniform density for each submanifold M_i can be defined as $p_i(\mathbf{x}) = \frac{1}{\pi}$ for all $\mathbf{x} \in M_i$.

Note that each of submanifolds are parametrized curves in \mathbb{R}^2 ,

$$\gamma_0: \theta \mapsto (\cos \theta, \sin \theta)$$

$$\gamma_1: \theta \mapsto (1 - \cos \theta, 1 - \sin \theta + 0.5)$$

with constant speed $\|\gamma_0'(\theta)\| = \|\gamma_1'(\theta)\| = 1$ at all $\theta \in [0, \pi]$. Therefore, from equation (2),

$$\int_{\mathbf{x}\in M_0} p|_{M_0}(\mathbf{x})dM_0(\mathbf{x}) = \int_{\theta=0}^{\pi} p(\gamma_0(\theta))d\theta$$

$$\int_{\mathbf{x}\in M_0} p|_{M_1}(\mathbf{x})dM_1(\mathbf{x}) = \int_{\theta=0}^{\pi} p(\gamma_1(\theta))d\theta$$
(4)

For any measurable subset $A \subseteq M$, the probability for an event that x is in A can be computed as follows.

$$\Pr[\mathbf{x} \in A] = \int_{\mathbf{x} \in A \subseteq M} p(\mathbf{x}) dM(\mathbf{x})$$

$$= \int_{\mathbf{x} \in A \cap M_0} p|_{M_0}(\mathbf{x}) dM_0(\mathbf{x}) + \int_{\mathbf{x} \in A \cap M_1} p|_{M_1}(\mathbf{x}) dM_1(\mathbf{x})$$

$$= \int_{\substack{\theta \in [0, \pi] \\ \gamma_0(\theta) \in A}} p|_{M_0}(\gamma_0(\theta)) d\theta + \int_{\substack{\theta \in [0, \pi] \\ \gamma_1(\theta) \in A}} p|_{M_1}(\gamma_1(\theta)) d\theta \quad (\because (4))$$

$$= \Pr[\mathbf{x} \in M_0] \int_{\substack{\theta \in [0, \pi] \\ \gamma_1(\theta) \in A}} p_0(\gamma_0(\theta)) d\theta$$

$$+ \Pr[\mathbf{x} \in M_1] \int_{\substack{\theta \in [0, \pi] \\ \gamma_1(\theta) \in A}} p_1(\gamma_1(\theta)) d\theta \quad (\because (3))$$

$$= \frac{1}{\pi} \left(\Pr[\mathbf{x} \in M_0] \int_{\substack{\theta \in [0, \pi] \\ \gamma_0(\theta) \in A}} 1 d\theta + \Pr[\mathbf{x} \in M_1] \int_{\substack{\theta \in [0, \pi] \\ \gamma_1(\theta) \in A}} 1 d\theta \right)$$

We can briefly check all the requirements (R1), (R2), and (R3). The computation of $\Pr[\mathbf{x} \in A]$ is bassed on (R1), so (R1) is satisfied trivially. Also, p is a function defined only on M, thus (R2) is clear, i.e. $\operatorname{supp}(p) = \{\mathbf{x} \in \mathbb{R}^n \mid p(\mathbf{x}) > 0\} \subseteq M$. To check (R3), when $A = M_i$, computing this integration will result in the exact probability $\Pr[\mathbf{x} \in M_i] = \Pr[y = i]$, so when A = M, computing the integration will result in $\Pr[y = 0] + \Pr[y = 1] = 1$, as desired in the requirements.

3.3 EXTENDING DENSITY

For a fixed point $\hat{\mathbf{x}} \in \mathbb{R}^n$, there is a family of density functions indexed by $\mathbf{x} \in M$ – the conditional density function $p_M(\hat{\mathbf{x}}|\mathbf{x}_o = \mathbf{x})$. The idea is to compute the density for compound distribution.

$$p_M(\hat{\mathbf{x}}) = \int_{\mathbf{x} \in M} p_M(\hat{\mathbf{x}} | \mathbf{x}_o = \mathbf{x}) p(\mathbf{x}) dM(\mathbf{x})$$

where p is the probability density function defined on M.

Due to the requirement (**R4**), the conditional density is equal to the translated noise density $\nu_{\mathbf{x}}(\hat{\mathbf{x}} - \mathbf{x})$. Therefore, we replace the conditional density by the translated noise density.

$$p_M(\hat{\mathbf{x}}) = \int_{\mathbf{x} \in M} \nu_{\mathbf{x}}(\hat{\mathbf{x}} - \mathbf{x}) p(\mathbf{x}) dM(\mathbf{x})$$
 (5)

Since $\nu_{\mathbf{x}}(\hat{\mathbf{x}} - \mathbf{x})$ is a function on \mathbf{x} when $\hat{\mathbf{x}}$ is fixed, computing this integration can be viewed as computing expectation of a real-valued function defined on M. Computing such expectation has been explored in detail Pennec (1999).

In the following section, an example extension will be provided. Also, in the section 3.6, the extension will be discussed further.

Extending density to \mathbb{R}^n Again, we will show an example that under a proper noise density function, we can construct the density with respect to M satisfying the requirement (R4). For simplicity, we choose isotropic Gaussian distribution, $\mathcal{N}(0,\sigma^2I)$ with standard deviation σ for each dimension, as the noise density function $\nu_{\mathbf{x}}$ for all $\mathbf{x} \in M$. Such noise density $\nu_{\mathbf{x}}$ defined in \mathbb{R}^n can be written as follows.

$$\nu_{\mathbf{x}}(\mathbf{n}_{\mathbf{x}}) = \frac{1}{\sqrt{2\pi}\sigma^2} \exp\left(-\frac{\parallel \mathbf{n}_{\mathbf{x}} \parallel_2^2}{2\sigma^2}\right)$$

By putting $\mathbf{n}_{\mathbf{x}} = \hat{\mathbf{x}} - \mathbf{x}$ to density equation above,

$$p_M(\hat{\mathbf{x}}) = \int_{\mathbf{x} \in M} \frac{1}{\sqrt{2\pi}\sigma^2} \exp\left(-\frac{\|\hat{\mathbf{x}} - \mathbf{x}\|_2^2}{2\sigma^2}\right) p(\mathbf{x}) dM(\mathbf{x})$$

Now, we visit our previous example of two-moons dataset again. We assume an isotropic Gaussian distribution with $\sigma = 0.05$ as the noise density $\nu_{\mathbf{x}}$ for all $\mathbf{x} \in M$.

By the equation (5), we have the following computation of density of $\hat{\mathbf{x}}$.

$$p_{M}(\hat{\mathbf{x}}) = \int_{\mathbf{x} \in M} \nu_{\mathbf{x}}(\hat{\mathbf{x}} - \mathbf{x}) p(\mathbf{x}) dM(\mathbf{x})$$

$$= \int_{\mathbf{x} \in M_{0}} \nu_{\mathbf{x}}(\hat{\mathbf{x}} - \mathbf{x}) p|_{M_{0}}(\mathbf{x}) dM_{0}(\mathbf{x}) + \int_{\mathbf{x} \in M_{1}} \nu_{\mathbf{x}}(\hat{\mathbf{x}} - \mathbf{x}) p|_{M_{1}}(\mathbf{x}) dM_{1}(\mathbf{x})$$

$$= \int_{\theta=0}^{\pi} \nu_{\mathbf{x}}(\hat{\mathbf{x}} - \mathbf{x}) p|_{M_{0}}(\gamma_{0}(\theta)) d\theta + \int_{\theta=0}^{\pi} \nu_{\mathbf{x}}(\hat{\mathbf{x}} - \mathbf{x}) p|_{M_{1}}(\gamma_{1}(\theta)) d\theta \quad (\because (2))$$

$$= \Pr[\mathbf{x} \in M_{0}] \int_{\theta=0}^{\pi} \nu_{\mathbf{x}}(\hat{\mathbf{x}} - \mathbf{x}) p_{0}(\gamma_{0}(\theta)) d\theta$$

$$+ \Pr[\mathbf{x} \in M_{1}] \int_{\theta=0}^{\pi} \nu_{\mathbf{x}}(\hat{\mathbf{x}} - \mathbf{x}) p_{1}(\gamma_{1}(\theta)) d\theta \quad (\because (3))$$

$$= \frac{1}{\pi \sqrt{2\pi}\sigma^{2}} \left[\Pr[\mathbf{x} \in M_{0}] \int_{\theta=0}^{\pi} \exp\left(-\frac{\|\hat{\mathbf{x}} - \mathbf{x}\|_{2}^{2}}{2\sigma^{2}}\right) d\theta \right]$$

$$+ \Pr[\mathbf{x} \in M_{1}] \int_{\theta=0}^{\pi} \exp\left(-\frac{\|\hat{\mathbf{x}} - \mathbf{x}\|_{2}^{2}}{2\sigma^{2}}\right) d\theta \right]$$

We can also check that the requirement $(\mathbf{R4})$ is satisfied by the construction; our construction (equation (5)) is based on $(\mathbf{R4})$.

3.4 GENERATIVE MODELS

A generative model tries to find a statistical model for joint density $p(\mathbf{x}, y)$ Ng & Jordan (2002). Equivalently, generative approach models the class-conditional density $p(\mathbf{x}|y)$ of generating data \mathbf{x} given a class y and the discrete distribution $\Pr[y=l]$ over the set of labels. Among different generative models, we are interested in a specific type transforming one distribution \mathcal{D}_Z to another distribution \mathcal{D}_X . In such generative models, latent vector $\mathbf{z} \sim \mathcal{D}_Z$ is sampled from a relatively simpler distribution, e.g. isotropic Gaussian. Then, a pre-trained deterministic function G maps to a sample $\mathbf{x} = G(\mathbf{z})$.

Specifically, we focus on *reversible generative models* as they facilitate the comparison between the density of generated samples and the target density. Unlike other approaches, reversible generative models take the dimensions of latent vectors to be same to the dimension of samples to be generated. This allows us to compute, for given \mathbf{x} , the density of its inverse image $\mathbf{z} = G^{-1}(\mathbf{x})$ by the *change of variable formula* relating the probability densities p_X , p_Z (of \mathcal{D}_X , \mathcal{D}_Z respectively).

$$p_X(\mathbf{x}) = p_Z(\mathbf{z}) \left| \det \left(\frac{\partial G(\mathbf{z})}{\partial \mathbf{z}^T} \right) \right|^{-1}$$
 (6)

whereas $\frac{\partial G(\mathbf{z})}{\partial \mathbf{z}^T}$ is the Jacobian of G which is as a mapping from \mathbb{R}^n to itself.

3.5 INVERT AND CLASSIFY (INC) APPROACH FOR ROBUST CLASSIFICATION

As the data generating manifold M contains class-wise disjoint submanifolds, there exists a classifier f on \mathbb{R}^n separating these submanifolds. For such f that separates submanifolds of M, any point classified incorrectly by f always lies out of M. Therefore, any adversary trying to change the classification of f would try pull a valid sample further out of manifold. By projecting incorrectly classified point to the neareast submanifold, we may expect the classification of f to be corrected by the projection. *Invert and Classify (INC)* method Ilyas et al. (2017) Samangouei et al. (2018) implements this intuition can be implemented by exploiting a pre-trained generative model.

The main idea of INC is to invert the perturbed sample by projecting to the nearest point on data generating manifold. Ideally, the data generating manifold M of the true distribution \mathcal{D}_X is accessible. For any point $(\hat{\mathbf{x}}, y)$ with $f(\hat{\mathbf{x}}) \neq y$, out-of-manifold perturbation is significantly reduced after projecting $\hat{\mathbf{x}}$ to \mathbf{x}^* on M as follows.

$$\mathbf{x}^* = \arg\min_{\mathbf{x} \in M} d(\mathbf{x}, \hat{\mathbf{x}}) \tag{7}$$

where d is a metric defined on the domain X. As perfect classification on M is assumed, if $\hat{\mathbf{x}}$ is close enough to the submanifold of correct label, classification $f(\hat{\mathbf{x}}^*)$ is likely to be correct, since \mathbf{x}^* is likely to be in the correct submanifold.

Since the manifold M is unknown in practice, a generative model G is trained to approximate the true distribution \mathcal{D}_X . The optimization with this approximated manifold is the INC approach.

$$\mathbf{x}^* = G(\mathbf{z}^*) \text{ where } \mathbf{z}^* = \arg\min_{\mathbf{z} \sim \mathcal{D}_Z} d(G(\mathbf{z}), \hat{\mathbf{x}})$$
 (8)

3.6 DISCUSSION ON THE EXTENDED DENSITY

Relation to kernel density estimation While this extension is computing the density of compound distribution, it can be interpreted as computing expectation over a family of locally defined densities. Such expected value can be observed in previous approaches of density estimation. For example, if $\nu_{\mathbf{x}}$ is isotropic Gaussian for each x, the above integration is equivalent to the kernel density estimation, with Gaussian kernel, over infinitely many points on M. We may also consider a set of multivariate Gaussian noises that are locally flattened to reflect the tangent space of manifold, the above integration is equivalent to density estimation using manifold parzen window Vincent & Bengio (2003).

Observed property of the extended density In Figure 1b in the Section 3.2, we can observe that the extended density achieved higher values near the data generating manifold. We formalize this observation to discuss about its implication to INC approach.

Let $d(\hat{\mathbf{x}}, M)$ to be the minimum distance from $\hat{\mathbf{x}}$ to the manifold M.

(C1) For any given $\hat{\mathbf{x}}$, let y^* be the class label whose conditional density $p_M(\hat{\mathbf{x}}|y=y^*)$ dominates $p_M(\hat{\mathbf{x}}|y=i)$ for $i \neq y^*$,

$$y^* \in \arg\max_{i \in [l]} p_M(\hat{\mathbf{x}}|y=i) \tag{9}$$

and let M_{y^*} be the submanifold corresponding to y^* .

(C2) For y^* satisfying (C1), we choose y^* such that the distance of $\hat{\mathbf{x}}$ from the manifold $d(\hat{\mathbf{x}}, M_{y^*})$ is the smallest.

If there are multiple y^* satisfying both of (C1) and (C2), we expect the following property to be true for all of those y^* .

(P1) Consider the shortest line from $\hat{\mathbf{x}}$ to the manifold M_{y^*} . As $\hat{\mathbf{x}}$ goes closer to M_{y*} along this line, $\hat{\mathbf{x}}$ should be more likely to be generated as the influence of noise decreases when moving away from the manifold. Therefore, we expect our density p_M to have the following property.

$$\mathbf{x}^* \in \arg\min_{\mathbf{x} \in M_{y^*}} d(\hat{\mathbf{x}}, \mathbf{x})$$

$$\Longrightarrow p_M(\hat{\mathbf{x}}) \le p_M((1 - \lambda)\hat{\mathbf{x}} + \lambda \mathbf{x}^*) \text{ for all } \lambda \in [0, 1]$$
(10)

Actually, this provides another justification of INC. In reality, the density conditioned by the label is not available even after running a generative model, so finding y^* with (C1) is relatively hard. If we only consider (C2) without filtering y^* via (C1), we are finding a point $\mathbf{x} \in M$ achieving the minimum distance to $\hat{\mathbf{x}}$, which is the optimization (7) above. Then projecting $\hat{\mathbf{x}}$ to the \mathbf{x}^* , i.e. the solution of the optimization 7, can be explained by 10; when $\lambda=1$, p_M is the highest along the shortest line between $\hat{\mathbf{x}}$ and \mathbf{x}^* .

4 TOPOLOGICAL PROPERTIES OF DATA FROM GENERATIVE MODELS

In this project, we explore the theory of generative model, especially about the differences in the topological properties of the latent vector distribution and the target distribution.

We mainly discuss that initial information, about the topology of target distribution¹, is crucial to the performance of the generative model. Specifically, if there are fundamental topological differences between the target distribution and the distribution of the latent vector, then any continous generative model G cannot approximate the target distribution properly.

¹The term topology of distirbutions refers to the topology of a shape that we will extract from distributions.

4.1 TOPOLOGY OF DISTRIBUTIONS BASED ON LEVEL SETS

Ideally, the data generating manifold is a geometric shape that corresponds to the distribution. However, the data generating manifold is not accessible in most cases, but we only have an indirect access to its extended distribution. Therefore, we try recovering a shape from the extended density, so that the "shape" successfuly approximates the data generating manifold.

 λ -density level set Use use the concept of λ -density level set Jiang (2017) to capture geometric features of the density function.

Definition 1 (λ -density level set). Let \mathcal{D} be a distribution on a space X, with density function p. Then, for a nonnegative λ , λ -density level set S_{λ} is defined as the inverse image of $[\lambda, \infty)$.

$$L_{p,\lambda} := p^{-1}[\lambda, \infty) = \{ \mathbf{x} \in X \mid p(\mathbf{x}) \ge \lambda \}$$

We provide the theorem about conditional existence of a λ -density level set reflecting the topological properties of the data generating manifold, under proper assumptions on noise density.

Assumptions on noise density We formally define the property of noise required. The intuition is that the influence of noise should diminish as observed sample $\hat{\mathbf{x}}$ moves away from a suspected source point \mathbf{x}_o . Therefore, we formalize the noise whose density decreases as the noise $\mathbf{n} = \hat{\mathbf{x}} - \mathbf{x}_o$ goes away from the origin.

Definition 2 (Center peaked noise density). A family of noise density functions $\nu_{\mathbf{x}}$ is *center peaked*, if for any source point $\mathbf{x} \in M$ and any noise vector $\mathbf{n} \in \mathbb{R}^n$ with $\|\mathbf{n}\| > 0$,

$$\nu_{\mathbf{x}}(\mathbf{n}) < \nu_{\mathbf{x}}(\lambda \mathbf{n}) \text{ for all } \lambda \in [0, 1)$$

Also, we do not expect high density for a large noise, e.g. uniform noise density over \mathbb{R}^n , so we require a notion of boundedness of noise density. We use the boundedness of λ -density level set of noise density (as a subset in \mathbb{R}^n) to formalize bounded family of noise densities.

Definition 3 (Level set bounded noise density). A family of noise densities $\nu_{\mathbf{x}}$ is *level set bounded*, if for any point \mathbf{x} and any threshold λ , if λ -density level set is nonempty, there exists a radius δ such that the closed ball of radius δ centered at origin contains the λ -density level set, i.e. $L_{\nu_{\mathbf{x}},\lambda} \subseteq \overline{B_{\delta}(\mathbf{0})}$.

where $\overline{B_{\delta}(\mathbf{0})}$ is the closed ball of radius δ centered at $\mathbf{0}$.

The definition 2 and the definition 3 induces the following radii.

Definition 4. Let $\nu_{\mathbf{x}}$ be a center peaked, level set bounded family of continuous noise densities. Let λ be a *small enough* threshold that $L_{\nu_{\mathbf{x}},\lambda}$ is nonempty for every \mathbf{x} .

We define a λ -bounding radius $\delta_{\mathbf{x},\lambda}$ to be the smallest δ that $\overline{B_{\delta}(\mathbf{0})}$ bounds the level set.

$$\delta_{\mathbf{x},\lambda} := \min\{\delta \mid L_{\nu_{\mathbf{x}},\lambda} \subseteq \overline{B_{\delta}(\mathbf{0})}\}\$$

Additionally, if $\max_{\mathbf{x} \in M} \delta_{\mathbf{x},\lambda}$ exists for some λ , we simply denote the maximum value as δ_{λ} .

Also, we define a λ -guaranteeing radius $\epsilon_{\mathbf{x},\lambda}$ as the largest ϵ that $B_{\epsilon}(\mathbf{0})$ is bounded by the level set,

$$\epsilon_{\mathbf{x},\lambda} := \max\{\epsilon \mid \overline{B_{\epsilon}(\mathbf{0})} \subseteq L_{\nu_{\mathbf{x}},\lambda}\}$$

Additionally, if $\min_{\mathbf{x}\in M} \epsilon_{\mathbf{x},\lambda}$ exists for a λ , we simply denote the minimum value as ϵ_{λ} .

We point out that these radii always exist under the conditions given in the definition 4.

Proposition 1. Any center peaked, level set bounded family of continuous noise densities $\nu_{\mathbf{x}}$ has both λ -bounding radius and λ -guaranteeing radius for λ such that $L_{\nu_{\mathbf{x}},\lambda}$ is nonempty for every \mathbf{x} .

Proof. Let $\nu_{\mathbf{x}}$ be a center peaked, level set bounded family of continuous noise densities. Since $\nu_{\mathbf{x}}$ is continuous, level set $L_{\nu_{\mathbf{x}},\lambda} = \nu_{\mathbf{x}}^{-1}[\lambda,\infty)$ is closed as an inverse image of $\nu_{\mathbf{x}}$. Therefore, it's boundary $\partial L_{\nu_{\mathbf{x}},\lambda}$ is contained in $L_{\nu_{\mathbf{x}},\lambda}$.

Because $\nu_{\mathbf{x}}$ is level set bounded, level set $L_{\nu_{\mathbf{x}},\lambda}$ is bounded by a closed ball $B_{\delta}(\mathbf{0})$ with radius $\delta \geq 0$. Since $\nu_{\mathbf{x}}$ is center peaked, a nonempty level set $L_{\nu_{\mathbf{x}},\lambda}$ always contains $\mathbf{0}$ as the maximum is achieved at $\mathbf{0}$. Moreover, there exists a closed neighborhood ball $\overline{B_{\epsilon}(\mathbf{0})}$ with radius $\epsilon \geq 0$ contained in the

level set $L_{\nu_x,\lambda}$. (: At least $\overline{B_0(\mathbf{0})} = \mathbf{0} \in L_{\nu_x,\lambda}$) Now it is enough to show that the minimum of δ and the maximum of ϵ exist.

Since $L_{\nu_{\mathbf{x}},\lambda}$ is bounded, its boundary $\partial L_{\nu_{\mathbf{x}},\lambda}$ is also bounded. $\partial L_{\nu_{\mathbf{x}},\lambda}$ is closed and bounded, thus it is a compact set. Therefore, the Euclidean norm, as a continuous function, should achieve the maximum \bar{r} and the minimum \underline{r} on $\partial L_{\nu_{\mathbf{x}},\lambda}$ by the extreme value theorem. From the choice of δ and ϵ , we can get,

$$\epsilon \leq \underline{r} \leq \overline{r} \leq \delta$$

Therefore, we can find the minimum $\delta_{\mathbf{x},\lambda} = \overline{r}$ and the maximum $\epsilon_{\mathbf{x},\lambda} = \underline{r}$.

The Definition 4 implies the following properties.

Lemma 1. Let $\nu_{\mathbf{x}}$ be a center peaked, level set bounded family of noise densities such that density $\nu_{\mathbf{x}}$ is continuous for every \mathbf{x} . If λ is *small enough* threshold that $L_{\nu_{\mathbf{x}},\lambda}$ is nonempty for every \mathbf{x} ,

$$\|\hat{\mathbf{x}} - \mathbf{x}\| > \delta_{\lambda} \implies \nu_{\mathbf{x}}(\hat{\mathbf{x}} - \mathbf{x}) < \lambda$$
$$\|\hat{\mathbf{x}} - \mathbf{x}\| < \epsilon_{\lambda} \implies \nu_{\mathbf{x}}(\hat{\mathbf{x}} - \mathbf{x}) > \lambda$$

Figure 2 shows an example of level set $L_{\mathbf{x},\lambda}$ of noise $\nu_{\mathbf{x}}$ at a point \mathbf{x} and its λ -bounding radius $\delta_{\mathbf{x},\lambda}$ and λ -guaranting radius $\epsilon_{\mathbf{x},\lambda}$.

Finally, we require noise density $\nu_{\mathbf{x}}$ to vary continuously as \mathbf{x} changes on the manifold M. While continuous variation may be defined in different ways², we require the continuity of both $\delta_{\mathbf{x},\lambda}$ and $\epsilon_{\mathbf{x},\lambda}$, as real-valued function of $\mathbf{x} \in M$ for a fixed value of λ .

Definition 5 (Continuously varying radii). A center peaked, level set bounded family of continuous noise densities $\nu_{\mathbf{x}}$ has *continuously varying radii* if, for a fixed λ that $L_{\nu_{\mathbf{x}},\lambda}$ is nonempty for every \mathbf{x} , λ -bounding radius $\delta_{\mathbf{x},\lambda}$ and λ -guaranteeing radius $\epsilon_{\mathbf{x},\lambda}$ are continous functions of \mathbf{x}

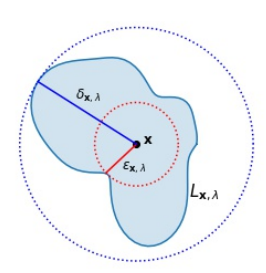


Figure 2: Example level set $L_{\mathbf{x},\lambda}$ with λ -bounding radius $\delta_{\mathbf{x},\lambda}$ and λ -guaranteeing radius $\epsilon_{\mathbf{x},\lambda}$.

When a family of noise densities has continuously varying radii, since we assume that the data generating manifold is compact, the extreme value theorem can be applied to $\delta_{\mathbf{x},\lambda}$ and $\epsilon_{\mathbf{x},\lambda}$. Therefore, both $\delta_{\lambda} = \max_{\mathbf{x} \in M} \delta_{\mathbf{x},\lambda}$ and $\epsilon_{\lambda} = \min_{\mathbf{x} \in M} \epsilon_{\mathbf{x},\lambda}$ exist in this case.

4.2 Main theorem

In this section, we will introduce the main theorem. The theorem will convey a message that, under the assumptions on noise densities from the Section 4.1, there exist a λ such that,

- (Inclusion) The λ -density level set $L_{p_M,\lambda}$ includes the data generating manifold M.
- (Separation) The λ -density level set $L_{p_M,\lambda}$ consists of connected components such that each component contains exactly one submanifold M_i .

Moreover, the separation is proved by showing that $L_{p_M,\lambda}$ is included by the neighborhood of M.

Definition 6 (ρ -neighborhood of manifold). Let X be a metric space equipped with a metric d, and let M be a manifold in X. For $\rho > 0$, a ρ -neighborhood of M is defined as,

$$N_{\rho}(M) := \{ \mathbf{x}' \mid \min_{\mathbf{x} \in M} d(\mathbf{x}, \mathbf{x}') < \rho \}$$

Before we proceed to the main theorem, we define concepts related to the data generating manifold.

Definition 7. Consider a data generating manifold M with density function p. For a radius $\epsilon > 0$, we define ω_{ϵ} to be the smallest probability of $\mathbf{x}' \in M$ being chosen in a ball $B_{\epsilon}(\mathbf{x})$ of radius ϵ , over the choice of the center $\mathbf{x} \in M$ of the ball.

$$\underline{\omega_{\epsilon}} := \min_{\mathbf{x} \in M} \Pr_{\mathbf{x}' \in M} [\mathbf{x}' \in B_{\epsilon}(\mathbf{x})]$$

²For example, Lipschitz continuity $\sup |\nu_{\mathbf{x}} - \nu_{\mathbf{x}'}| < \kappa \cdot d_g(\mathbf{x}, \mathbf{x}')$, where d_g is the geodesic distance induced from Riemaniann metric g.

This value depends on the local geometry of data generating manifold M, and is used as an important parameter to determine the lower bound of λ for inclusion.

Also, we define the *class-wise distance* of the data generating manifold M. Since the data generating manifold M consists of submanifolds M_1, \ldots, M_l corresponding to class labels, we can consider the pairwise distances for each pair of submanifolds M_i and M_j . We define the minimum class-wise distance to be the smallest pairwise distance between any pair of submanifolds.

Definition 8 (Class-wise distance of data generating manifold). Let X be a metric space equipped with a metric d, and let $M = \bigcup_{i=1}^{l} M_i$ be a data generating manifold in X. The class-wise distance of M is defined as,

$$\min_{\substack{i,j \in [l] \\ i \neq j}} \min_{\mathbf{x} \in M_i} d(\mathbf{x}, \mathbf{x}')$$

This distance actually captures the distance between the most confusing pair of class labels. If the noise density is not bounded properly, it is harder to have separation in the extracted shape for the majority of data.

Now, we present the main theorem. To begin with, pick a value λ such that the λ -density level set $L_{\nu_{\mathbf{x}},\lambda}$ is nonempty for all $\mathbf{x} \in M$. As we use noise densities $\nu_{\mathbf{x}}$ described in Section 4.1, both λ -bounding radius $\delta_{\lambda} = \max_{\mathbf{x} \in M} \delta_{\mathbf{x},\lambda}$ and λ -guaranteeing radius $\epsilon_{\lambda} = \min_{\mathbf{x} \in M} \epsilon_{\mathbf{x},\lambda}$ exist.

Then, we can prove the following lemma for the inclusion part.

Lemma 2. Assume a family of noise densities satisfies the assumptions of the Section 4.1. Let $\lambda > 0$ be a value such that the λ -density level set $L_{\nu_{\mathbf{x}},\lambda}$ is nonempty for any $\mathbf{x} \in M$. Also, let $\epsilon = \epsilon_{\lambda}$ be the minimum λ -guaranteeing radius over M. Then, for any $\mathbf{x} \in M$, the extended density value is at least $\omega_{\epsilon}\lambda$, i.e. $p_M(\mathbf{x}) \geq \omega_{\epsilon}\lambda$

Proof. By Lemma 1,

$$\mathbf{x}' \in B_{\epsilon}(\mathbf{x}) \iff \mathbf{x} \in B_{\epsilon}(\mathbf{x}') = B_{\epsilon_{\lambda}}(\mathbf{x}') \quad (\because \epsilon = \epsilon_{\lambda})$$

$$\implies \nu_{\mathbf{x}'}(\mathbf{x} - \mathbf{x}') > \lambda$$

Then, we can lower bound the density $p_M(\mathbf{x})$ as follows.

$$p_{M}(\mathbf{x}) = \int_{\mathbf{x}' \in M} \nu_{\mathbf{x}'}(\mathbf{x} - \mathbf{x}') p(\mathbf{x}') dM(\mathbf{x}')$$

$$\geq \int_{\mathbf{x}' \in M \cap B_{\epsilon}(\mathbf{x})} \nu_{\mathbf{x}'}(\mathbf{x} - \mathbf{x}') p(\mathbf{x}') dM(\mathbf{x}')$$

$$\geq \lambda \int_{\mathbf{x}' \in M \cap B_{\epsilon}} p(\mathbf{x}') dM(\mathbf{x}')$$

$$= \lambda \Pr_{\mathbf{x}' \in M} [\mathbf{x}' \in B_{\epsilon}(\mathbf{x})]$$

$$\geq \omega_{\epsilon} \lambda$$

This lemma shows that the thresholding the extended density p_M with threshold $\lambda^* \leq \omega_{\epsilon} \lambda$ guarantees the level set to include the entire manifold M.

Corollary 1. For any threshold $\lambda^* \leq \omega_{\epsilon} \lambda$, the corresponding λ^* -density level set L_{p_M,λ^*} of the extended density p_M includes the data generating manifold M.

Similarly, we provide the following lemma for the separation part.

Lemma 3. Assume a family of noise densities satisfies the assumptions of the Section 4.1. Let $\lambda > 0$ be a value such that the λ -density level set $L_{\nu_{\mathbf{x}},\lambda}$ is nonempty for any $\mathbf{x} \in M$. Also, let $\delta = \delta_{\lambda}$ be the maximum λ -bounding radius over M. Then, for any $\hat{\mathbf{x}} \notin N_{\delta}(M)$, the extended density value is smaller than λ , i.e. $p_M(\hat{\mathbf{x}}) < \lambda$.

Proof. By Lemma 1,

$$\hat{\mathbf{x}} \notin N_{\delta}(M) \iff \hat{\mathbf{x}} \notin B_{\delta}(\mathbf{x}) = B_{\delta_{\lambda}}(\mathbf{x}) \text{ for any } \mathbf{x} \in M \quad (\because \delta = \delta_{\lambda})$$

 $\implies \nu_{\mathbf{x}}(\hat{\mathbf{x}} - \mathbf{x}) < \lambda \text{ for any } \mathbf{x} \in M$

Then, we can upper bound the density $p_M(\hat{\mathbf{x}})$ as follows.

$$\begin{split} p_{M}(\hat{\mathbf{x}}) &= \int_{\mathbf{x} \in M} \nu_{\mathbf{x}} (\hat{\mathbf{x}} - \mathbf{x}) p(\mathbf{x}) dM(\mathbf{x}) \\ &< \lambda \int_{\mathbf{x} \in M} p(\mathbf{x}) dM(\mathbf{x}) \quad (\because \hat{\mathbf{x}} \not\in N_{\delta_{\lambda}}(M)) \\ &= \lambda \end{split}$$

This lemma says that, the λ -density level set is included by the δ -neighborhood $N_{\delta}(M)$ of the data generating manifold M.

Now, we can deduce the following main result.

Theorem 1. Pick any $\lambda^* \leq \omega_{\epsilon} \lambda$ threshold value satisfying the Corollary 1. If the class-wise distance of data generating manifold is larger than $2\delta^*$ where $\delta^* = \delta_{\lambda^*}$ (the λ^* -bounding radius), then the level set L_{p_M,λ^*} satisfies the followings.

- L_{p_M,λ^*} contains the data generating manifold M.
- Each connected component of L_{p_M,λ^*} contains at most one submanifold M_i of class i.

Proof. The first property is a direct application of Corollary 1 for $\lambda^* = \omega_{\epsilon} \lambda$.

For the Second property, since the class-wise distance of M is larger than $2\delta^*$, the δ^* -neighborhood of submanifolds are pairwise disjoint, i.e. $N_{\delta^*}(M_i) \cap N_{\delta^*}(M_j) = \emptyset$ for each $i \neq j$. Therefore, $N_{\delta^*}(M)$ has exactly k connected components that are $N_i = N_{\delta^*}(M_i)$'s.

By Lemma 3, δ^* -neighborhood $N_{\delta^*}(M)$ contains the level set L_{p_M,λ^*} , thus each connected component of L_{p_M,λ^*} is in exactly one of N_i 's. Since M is contained in L_{p_M,λ^*} , each M_i is contained in some connected component C of L_{p_M,λ^*} which is in N_i , i.e. $M_i \subset C \subset N_i$. Now, we need to show that such C containing a submanifold M_i can never contain any other submanifold M_j for $j \neq i$.

For any $j \neq i$, the corresponding submanifold $M_j \subset N_j$ is disjoint to N_i , because N_i and N_j are disjoint. This implies that M_j does not intersect with $C \subset N_i$. Therefore, if a connected component C contains a submanifold M_i , then it cannot contain any other submanifold.

4.3 APPLICATION TO THE GENERATIVE MODEL

In this section, all the conditions used in the Theorem 1 are assumed to show an application of generative model. We use the following notations for the distributions are of interest.

- \mathcal{D}_X : Target distribution to be approximated by using the generative model G
- \mathcal{D}_Z : Distribution of latent vectors, relatively simpler than \mathcal{D}_X , e.g. isotropic Gaussian.
- $\mathcal{D}_{G(Z)}$: Distribution of function values of G, given the distribution of latent vectors \mathcal{D}_Z .

For each of the distributions, we denote the λ -density level set of densities by L_{λ}^{X} , L_{λ}^{Z} , and $L_{\lambda}^{G(Z)}$, respectively. Note that $\mathcal{D}_{G(Z)}$ is the distribution of samples generated by G, so the performance of the generative model depends on the difference between $\mathcal{D}_{G(Z)}$ and \mathcal{D}_{X} .

Also, we assume the generative model G to be continuous. By assuming continuity of G, we can focus on the topological properties of the \mathcal{D}_Z instead of $\mathcal{D}_{G(Z)}$, as continuous map preserves some topological properties, e.g. the number of connected components. More precisely, if G is continuous, $L_{\lambda}^{G(Z)} = G(L_{\lambda}^Z)$ inherits the topological properties of L_{λ}^Z ; thus comparing L_{λ}^X and L_{λ}^Z is sufficient to observe the discrepancy between \mathcal{D}_X and $\mathcal{D}_{G(Z)}$.

The following theorem states that if one starts from improper initial information about the target distribution, L_λ^X and $L_\lambda^{G(Z)}$ do not agree on their number of connected components.

Theorem 2. Let \mathcal{D}_Z be a mixture of n_Z multivariate Gaussian distributions, and let \mathcal{D}_X be the target distribution generated from a data generating manifold with n_X submanifolds. Let G be a continuous generative model for \mathcal{D}_X using latent vectors from \mathcal{D}_Z . Assume the Theorem 1 is satisfied, and let λ^* be the threshold value from the Theorem 1.

If $n_Z < n_X$, $L_{\lambda^*}^X$ and $L_{\lambda^*}^{G(Z)}$ do not agree on the number of connected component.

Proof. Since $L_{\lambda^*}^X$ is the results of Theorem 1, the number of connected component of $L_{\lambda^*}^X$ is at least n_X .

However, sicne \mathcal{D}_Z is a mixture of Gaussians, for any value of λ (including the special case $\lambda=\lambda^*$), L^Z_λ can never have more than n_Z connected components. Since G is continuous, it preserves the number of connected components, thus $L^{G(Z)}_{\lambda^*}=G(L^Z_{\lambda^*})$ has at most n_Z connected components. As $n_Z < n_X$, $L^X_{\lambda^*}$ and $L^{G(Z)}_{\lambda^*}$ can never agree on the number of connected components. \square

This theorem is sufficient to deduce a corollary explaining why INC approach may fail when generative model is trained with an improper initial information.

Corollary 2. If Theorem 2 is satisfied, there is a point $\hat{\mathbf{x}} \in \mathbb{R}^n$ such that $\hat{\mathbf{x}} \notin L_{\lambda^*}^X$ but $\hat{\mathbf{x}} \in L_{\lambda^*}^{G(Z)}$.

Proof. Since $n_Z < n_X$, there exists a connected components \hat{C} of $L_{\lambda^*}^{G(Z)}$ containing at least two connected components of $S_{\lambda^*}^X$. Without loss of generality, assume \hat{C} contains exactly two connected components C and C'. By definition, λ -level set is a closed set, so C and C' are disjoint closed set. In Euclidean space \mathbb{R}^n , the Urysohn lemma tells us that for any disjoint pair of closed sets A, A' in \mathbb{R}^n , there is a continuous function f such that $f|_A(\mathbf{x}) = 0$ and $f|_{A'}(\mathbf{x}) = 1$ for any $\mathbf{x} \in \mathbb{R}^n$. Especially, when A = C and A' = C', there exists a continuous function f such that,

- $f(\mathbf{x}) = 0$ for all \mathbf{x} in C
- $f(\mathbf{x}) = 1$ for all \mathbf{x} in C'

Consider $S=f^{-1}(\frac{1}{2})$ which is a separating plane separating C and C'. If $\hat{C}\cap S=\emptyset$, then $\hat{C}\cap f^{-1}[0,\frac{1}{2})$ and $\hat{C}\cap f^{-1}(\frac{1}{2},1]$ will be two open set in subspace \hat{C} , whose union is \hat{C} . This implies that \hat{C} is disconnected, which is a contradiction. Therfore, $\hat{C}\cap S$ should be nonempty, and any point \mathbf{x} in $\hat{C}\cap S$ is not in $L^X_{\lambda^*}$.

This corollary tells us the existence of latent vector \mathbf{z} in the λ^* -level set of \mathcal{D}_Z , such that the generated sample $G(\mathbf{z})$ is not in the λ^* -level set of \mathcal{D}_X . In other words, with density at least λ^* , the generative model generates a point $G(\mathbf{z})$ which is unlikely to be generated by the target distribution. Since INC is based on searches over Z, this shows the potential drawback of the INC method, e.g. output an out-of-manifold point as a solution of optimization (8).

In the following section, the Theorem 2 is generalized for more topological properties.

4.4 Generalization of the Theorem 2

The Theorem 2 mainly uses a fact that the number of connected components of λ -density level set is preserved by continous generative model G.

In algebraic topology, each connected component corresponds to a generator of 0-th homology group H_0 , and continuity of a function is enough to preserve each components. In general, generators of i-th homology group H_i for i>0 are not preserved by a continuous map, so we need to restrict G further. By requiring G to be a homeomorphism, we can safely guarantee that all topological properties are preserved by G, therefore we can generalize the Theorem 2 with a homeomorphic generative model G.

To generalize the proof of the Theorem 2, we first provide the sketch of the proof.

(1) λ^* -density level set $L^Z_{\lambda^*}$ of mixture of Gaussian has at most n_Z connected component.

- (2) Since G is continuous, the number of connected components of $L_{\lambda^*}^G(Z) = G(L_{\lambda^*}^Z)$ is same to the number of connected components of $L_{\lambda^*}^Z$, so it is also at most n_Z .
- (3) We chose λ^* so that $L_{\lambda^*}^X$ is included in δ^* -neighborhood of M.
- (4) By assumption on the class-wise distance of M, δ^* -neighborhood of M has exactly same number of connected components to M, i.e. n_X . Therefore $L_{\lambda^*}^X$ has at least n_X connected components.
- (5) By (2) and (4), we conclude that $L_{\lambda^*}^G(Z)$ and $L_{\lambda^*}^X$ do not agree on the number of connected components as long as $n_Z < n_X$.

In this proof, n_Z corresponds to the maximal 0-th Betti number of $L^Z_{\lambda^*}$, i.e. the number of generators of $H_0(L^Z_{\lambda^*})$. If we keep using mixture of Gaussian as latent vector distribution, all component of $L^Z_{\lambda^*}$ are contractible, so we may use 0 as the maximal i-th Betti number.

Also, n_X corresponds to the 0-th Betti number of M and it worked as the minimal 0-th Betti number of $L_{\lambda^*}^X$. The condition on the class-wise distance of M is used to ensure n_X to be a lower bound. Combining these observations, we can ge the following generalized statement.

Theorem 3. Let \mathcal{D}_Z be a mixture of multivariate Gaussian distributions, and let \mathcal{D}_X be the target distribution from data generating manifold M. Let n_i be the i-th Betti number of M.

Consider a generative model G is used to approximate \mathcal{D}_X using the latent vectors sampled from \mathcal{D}_Z . Assume that G is a homeomorphism from \mathbb{R}^n to itself. Assume that data generating manifold satisfies the conditions of the Theorem 1, and let λ^* be the threshold value that $L_{\lambda^*}^X$ corresponds to that level set. Assume that for some j>0, the homomorphism ι^* induced by the inclusion $\iota:M\to N_{\delta^*}(M)$ is injective. 3

If $0 < n_j, L_{\lambda^*}^X$ and $L_{\lambda^*}^{G(Z)}$ do not agree on the number of connected component.

Proof. Since $L_{\lambda^*}^X$ is the results of Theorem 1, it includes M and is included by δ^* -neighborhood $N_{\delta^*}(M)$ of M. Define inclusions ι_1, ι_2 as,

- $\iota_1: M \to L^X_{\lambda^*}$
- $\iota_2: L^X_{\lambda^*} \to N_{\delta^*}(M)$

Clearly, $\iota = \iota_2 \circ \iota_1$.

Let ι_1^* and ι_2^* be induced homomorphisms of ι_1 and ι_2 , resp.

By the assumption, any generator [a] in $H_j(M)$ is injectively mapped to a nonzero generator $\iota^*([a])$ in $H_j(N_{\delta^*}(M))$. Therefore, the j-th Betti number of $N_{\delta^*}(M)$ is equal to that of M, i.e. n_j . Note that j-th Betti number is the rank of j-th homology group $\operatorname{rank}(H_j(N_{\delta^*}(M)))$ Because ι_2^* is a homomorphism from $H_j(L_{\lambda^*}^X)$ to $H_j(N_{\delta^*}(M))$, $\operatorname{rank}(L_{\lambda^*}^X) \geq \operatorname{rank}(H_j(N_{\delta^*}(M)))$. Therefore the j-th Betti number of $L_{\lambda^*}^X$ is at least n_j .

However, sicne \mathcal{D}_Z is a mixture of Gaussians, for any value of λ (including the special case $\lambda = \lambda^*$), L^Z_λ does not have any generator of j-th homology group, so it has j-th Betti number 0 for all j>0. Since G is homeomorphic, it preserves all the Betti numbers, thus $L^{G(Z)}_{\lambda^*} = G(L^Z_{\lambda^*})$ has the same j-th Betti number. As $0 < n_j$, $L^X_{\lambda^*}$ and $L^{G(Z)}_{\lambda^*}$ can never agree on the number of connected components. \square

Later in Section 5.2, we will see the Figure 4f from the circles dataset, which is a remarkable example that $L_{\lambda}^G(Z)$ has the same number of connected components, but does not have any loop (non-contractible circle). This is an empirical evidence of the Theorem 3, so it is explained by mismatches in the topology of distributions. Each concentric circle has $\mathbb Z$ as its first homology group as circle contains exactly one generator. However, latent vector distribution always has trivial first homology group, as any level set of mixture of gaussian is a set of contractible connected components.

³Any generator of the j-th homology group $H_j(M)$ of M is mapped to a nonzero generators of the j-th homology group $H_j(N_{\delta^*}(M))$ of δ^* -neighborhood of M.

5 EXPERIMENTAL RESULT

In this section we provide an empirical verification of theorems, and exploration of INC performance according to what the theorems imply. Our main goal are to check (1) the correctness of Theorem 2 and Corollary 2 for toy datasets, and (2) the improvement in INC performance when generative model is trained properly with initial information. To be specific, the following list shows the three main questions to be answered in this section.

- (Q1) Can we experimentally verify the results of section 4.3, in terms of the quality of generative model?
- (Q2) How does INC projection fail when generative model is not aware of topology information?
- (Q3) Does the topology-aware generative model improve the INC performance?

Experimental highlights In summary, we found out the following observations:

- (A1) Theorem 2 and Corollary 2 can be verified by plotting λ -density level set. Especially, we visualize the λ -density level set of $\mathcal{D}_{G(Z)}$ reflecting Theorem 2 and Corollary 2.
- (A2) When generative model is not trained with topology information, naive INC may fail. We found out two possible reasons regarding INC failure: (1) choice of bad initial point and (2) out-of-manifold search due to non-separation of density level set.
- (A3) The performance of INC can be improved by training a generative model with information about the topology of the target distribution. To elaborate, after training a generative model with additional information on the topology of the target distribution, we improved the average performance of INC by decreasing the error induced by projection to 30% of the topology-ignorant counterpart.

In the rest of this section, we provide more detailed description of our experiments. First, we begin with describing the details of experimental setup in section 5.1: datasets, latent vector distributions, generative model architecture, and INC implementation. Then, section 5.2-5.4 will describe the experimental results regarding each of the findings summarized above.

5.1 EXPERIMENTAL SETUP

Datasets For all experiments in this project, we used three small datasets in \mathbb{R}^2 : two-moons, spirals, and circles. Two-moons and circles are common example datasets included in a sampling module of Scikit-learn package. Spirals dataset was inspired by one of the toy datasets in FFJORD implementation Grathwohl et al. (2018), while we changed it from arithmetic spirals to logarithmic spirals to facilitate the uniform sampling from each manifolds.

Two-moons dataset is a set of submanifolds corresponding to two half-circles with the lower half-circle translated by (1,0.5). This dataset is used as an exemplary dataset due to its simplicity, and is also used in our example density computation in section 3.2 and 3.3.

$$M_{0} = \left\{ (x_{1}, x_{2}) \middle| \begin{array}{l} x_{1} = \cos \theta \\ x_{2} = \sin \theta \end{array} \text{ for } \theta \in [0, \pi] \right\}$$

$$M_{1} = \left\{ (x_{1}, x_{2}) \middle| \begin{array}{l} x_{1} = 1 - \cos \theta \\ x_{2} = 1 - \sin \theta + \frac{1}{2} \end{array} \text{ for } \theta \in [0, \pi] \right\}$$

Spirals dataset is a set of submanifolds corresponding to three logarithmic spirals. This dataset is chosen to check our hypothesis for dataset with more than two labels.

$$\begin{split} M_0 &= \left\{ (x_1, x_2) \middle| \begin{array}{l} x_1 &= \frac{1}{3}e^t \cos(t) \\ x_2 &= \frac{1}{3}e^t \cos(t) \end{array} \right. \text{ for } t \in [0, T] \right\} \\ M_1 &= \left\{ (x_1, x_2) \middle| \begin{array}{l} x_1 &= \frac{1}{3}e^t \cos(t + \frac{2}{3}\pi) \\ x_2 &= \frac{1}{3}e^t \sin(t + \frac{2}{3}\pi) \end{array} \right. \text{ for } t \in [0, T] \right\} \\ M_2 &= \left\{ (x_1, x_2) \middle| \begin{array}{l} x_1 &= \frac{1}{3}e^t \cos(t + \frac{4}{3}\pi) \\ x_2 &= \frac{1}{3}e^t \sin(t + \frac{4}{3}\pi) \end{array} \right. \text{ for } t \in [0, T] \right\} \end{split}$$

where T is set to be $\ln\left(\frac{15}{\sqrt{2}}+1\right)$. The dataset is scaled down by a factor $\frac{1}{3}$ to reduce its diameter.

⁴ The choice is due to the reparametrization by arc length s by setting $t = \ln\left(\frac{s}{\sqrt{2}} + 1\right)$ for $s \in [0, 15]$. With the reparametrization, uniform sampling of s guarantees uniform sampling over the manifold M.

Circles dataset is a set of submanifolds corresponding to two concentric circles. This dataset is chosen to check the result for dataset with nontrivial first homology group; the corresponding shape contains at least one non-contractible cycle.

$$M_{0} = \left\{ (x_{1}, x_{2}) \middle| \begin{array}{l} x_{1} = \cos \theta \\ x_{2} = \sin \theta \end{array} \right. \text{ for } \theta \in [0, 2\pi] \right\}$$

$$M_{1} = \left\{ (x_{1}, x_{2}) \middle| \begin{array}{l} x_{1} = \frac{1}{2} \cos \theta \\ x_{2} = \frac{1}{2} \sin \theta \end{array} \right. \text{ for } \theta \in [0, 2\pi] \right\}$$

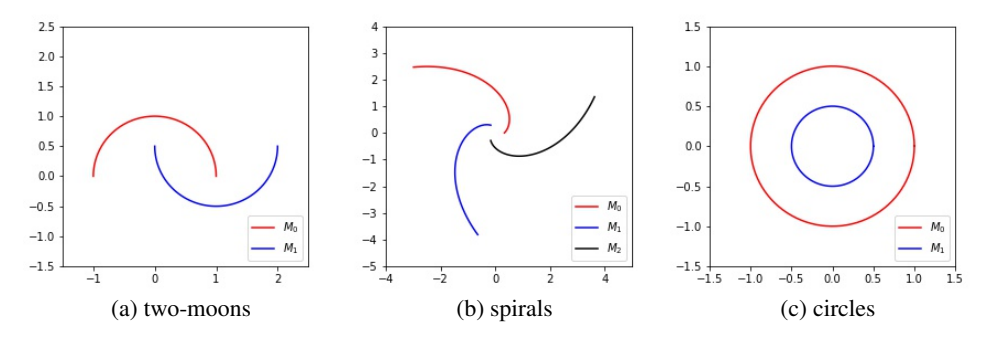


Figure 3: Data generating manifolds used in the experiments

To construct the training set, we first sampled 1000 points uniformly from each submanifold M_i , then each point was perturbed by isotropic Gaussian noise with standard deviation $\sigma = 0.05$. Before the training, each training set was standardized by a preprocessing function of Scikit-learn package.

Latent vector distributions For latent vector distributions \mathcal{D}_Z , we prepared three different mixtures of n_Z Gaussian distributions with $n_Z = 1, 2, 3$.

When $n_Z=1$, \mathcal{D}_Z is an isotropic Gaussian centered at $\mu=0$ with standard deviation $\sigma=1$. When $n_Z=2,3$, we arranged n Gaussian distributions along a circle of radius R=2.5, so that i-th Gaussian has mean at $\mu_i=\left(-R\sin\left(\frac{2\pi i}{n}\right),R\cos\left(\frac{2\pi i}{n}\right)\right)$ with $\sigma=0.5$ for n=2 and $\sigma=0.3$ for n=3. Then, we used the uniform mixture of the arranged Gaussian was used as \mathcal{D}_Z .

5.2 VISUAL VERIFICATION OF THEOREMS

The goal of this section is to verify the Theorem 2 and the Corollary 2, by visualizing the level set reflecting the theorem statements. We also compare two versions of generative models in terms of the separation of level sets.

Figure 4 shows the λ -density level sets of densities of $\mathcal{D}_{G(Z)}$ using the same threshold $\lambda=0.01$. The first row and the second row show the results from the class-ignorant version and the class-aware version, respectively. Each column corresponds to the level set for each dataset. All distributions are scaled due to the standardization preprocessing before the training.

In general, we can observe separations of level set components when the generative model is class-aware. On the contrary, for the class-ignorant generative models, we can observe connections between level set components, which was expected by the Corollary 2. Due to this connection, the class-ignorante generative models achieves less number of connected component in its level set, and this verifies the Theorem 2 for our choice of $\lambda^* = 0.01$.

5.3 INC FAILURE DUE TO THE LACK OF INFORMATION ABOUT THE TOPOLOGY OF THE DISTRIBUTION

Now we present how the non-separation of level set, shown in the section 5.2, influences the performance of the INC projection. We provide two possible explanations of why INC may fail in contrast with its promising theoretical descriptions. First, it is pointed out that bad initialization causes INC to output suboptimal solution on a submanifold different from the nearest manifold. Also, we point out that the artifact, induced by the topological difference of level sets, makes INC search out of manifold, resulting the out-of-manifold solution as an output. Finally, we demonstrate the

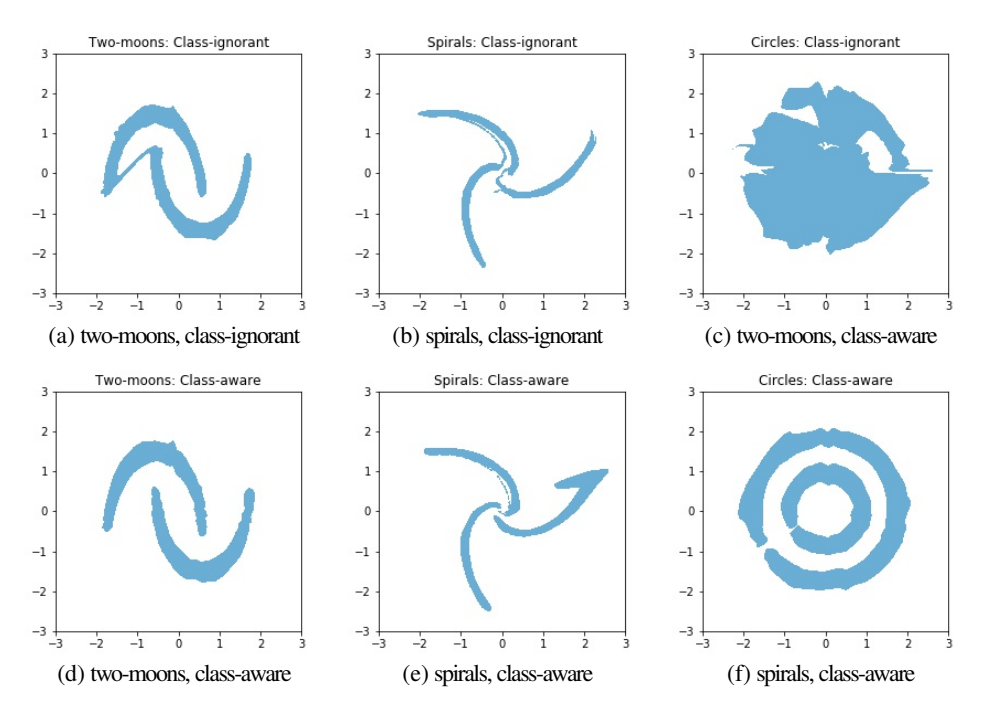


Figure 4: λ -density level sets of $\mathcal{D}_{G(Z)}$ with $\lambda = 0.01$

effect of the level set differences on general INC performances when INC is applied to improve the robustness of an ill-trained model.

Figure 5 are three visualized examples of INC with class-ignorant generative model for two-moons. In each plot, black dot is the given point \hat{x} , and blue dot is the initial point from choosing z randomly from the latent vector distribution – a single mode isotropic Gaussian in this case, and red dot is the final point returned by INC. All intermediate points during the optimization are plotted with smaller dots with colors gradually changing from blue to red. Training set of two-moon used in generative model training was plotted and blurred for visualization.

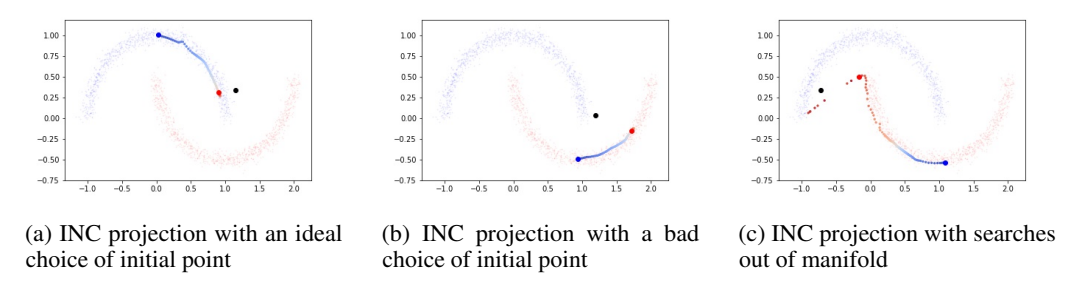


Figure 5: Successful and failed cases of INC using class-ignorant generative model of two-moon. The Figure 5a is the ideal example of INC projection. In this case, The initial point was chosen the the same manifold to the manifold that is closest to $\hat{\mathbf{x}}$. Then, the INC optimization searches along the manifold until the it reaches to a point close enough to $\hat{\mathbf{x}}$.

The Figure 5b shows the case that INC failed because it started from a bad initial point. We can observe that the initial point was chosen on the other submanifold than the submanifold where the desired solution lies, then the INC converged to a local optimum on the wrong submanifold. We point out that this is inevitable as the class-ignorant type INC does not have an ability to choose a random initial point in a desired submanifold.

The Figure 5c shows another case that INC failed. Here, not only that INC converged in a wrong manifold, but we can observe a nontrivial amount of intermediate points out of manifold during the optimization. This set of points suggests that INC may end up with an out-of-manifold solution.

Finally, we present experiments to demonstrate the effect of the level set discrepency on the INC performance. First, we begin with training support vector machines (SVMs) performing classification tasks for our target distributions. For training data, we randomly sampled 1000 training points from each data generating manifold. The baseline SVMs were intentionally ill-trained, by using high kernel coefficient $\gamma=100$. ⁵ After training SVMs, we form other classifiers by applying INC to ill-trained SVMs To explain, for each dataset, we have four types of classifiers as follows.

- 1. Ill-trained SVM: Baseline classifier
- 2. Ideal INC: Classfier with INC with a direct access to the data generating manifolds
- 3. Class-ignorant INC: Classfier with INC with data distribution approximated by a class-ignorant generative model
- 4. Class-aware INC: Classfier with INC with data distribution approximated by a class-aware generative model

We want to emphasize that a direct access to the data generating manifold is not possible in general. However, applying INC based on such direct access gives us an INC purely based on the geometry, so it is an ideal form of INC that should be approximated. Also, since class-ignorant is affected by bad choice of initial point, we reduce the effect of bad initalization by sampling more initial points and taking the best solution among the projection results. For this number of initial choices, we chose initial points as many as the number of manifolds, which is exactly same to the number of initial points for class-aware INC model.

To demonstrate the improvement in the robustness of the model, we visualize the effect by depicting the decision boundary of each classfier. To be specific, we form a 300×300 grid on the domain of $[-3,3] \times [-3,3]$, then compute the result of classification. The depicted decision boundaries are presented in the Figure 6. Each row corresponds to each dataset: two moons, spirals, and circles, respectively. Each column corresponds to classifier 1-4 described above, from the first column to the fourth column, respectively. From the Figure 6, it is visually evident that class-aware INC models provide more proper approximations to the ideal INC model.

5.4 INC IMPROVEMENT VIA CLASS-AWARE GENERATIVE MODEL

In the final part of our experiments, we demonstrate that INC performance is improved by using class-aware generative models.

To measure the performance of INC, we first choose 100 points from each submanifold M_i by uniformly dividing the closed interval of parameter. Then each point \mathbf{x} is perturbed by a vector $\mathbf{n}_{\mathbf{x}}$ normal to the submanifold at \mathbf{x} , generating 200 adversarial points $\hat{\mathbf{x}} = \mathbf{x} \pm r \, \mathbf{n}_{\mathbf{x}}$. For all of the datasets, we used r = 0.2 for perturbation size. We run two types of INC, expecting INC to map $\hat{\mathbf{x}}$ back to the original point \mathbf{x} , as \mathbf{x} is the solution to the optimization (7). We define the *projection error* of INC as $\|\mathrm{INC}(\hat{\mathbf{x}}) - \mathbf{x}\|_2$, and collect the statistics of projection errors over all $\hat{\mathbf{x}}$. All generative model is trained over standardized data, but we measured the projection errors in the original scale of the dataset.

Two-moons		Spirals		Circles	
class-ignorant	class-aware	class-ignorant	class-aware	class-ignorant	class-aware
0.647 (0.666)	0.148 (0.208)	1.523 (1.338)	0.443 (0.440)	0.699 (0.491)	0.180 (0.259)

Table 1: Comparison of the projection errors of INC based on the class-awareness of the model.

Table 1 shows the statistics of the projection errors when INC is implemented using class-ignorant generative model and class-aware generative model. Each pair of columns provides the results on the dataset written at the top row. For each pair of columns, one column shows the INC performance with class-ignorant generative model, where the other column shows with class-aware version. Numbers in each cell are mean and standard deviation (in parenthesis) of the projection error. For all of the datasets, when class-aware models were used, the projection errors became significantly lower than the projection error incurred by the class-ignorant counterpart.

 $^{^5}$ In general, choosing unnecessarily high kernel coefficient γ causes overfitting, inducing decision boundary close to the training data.

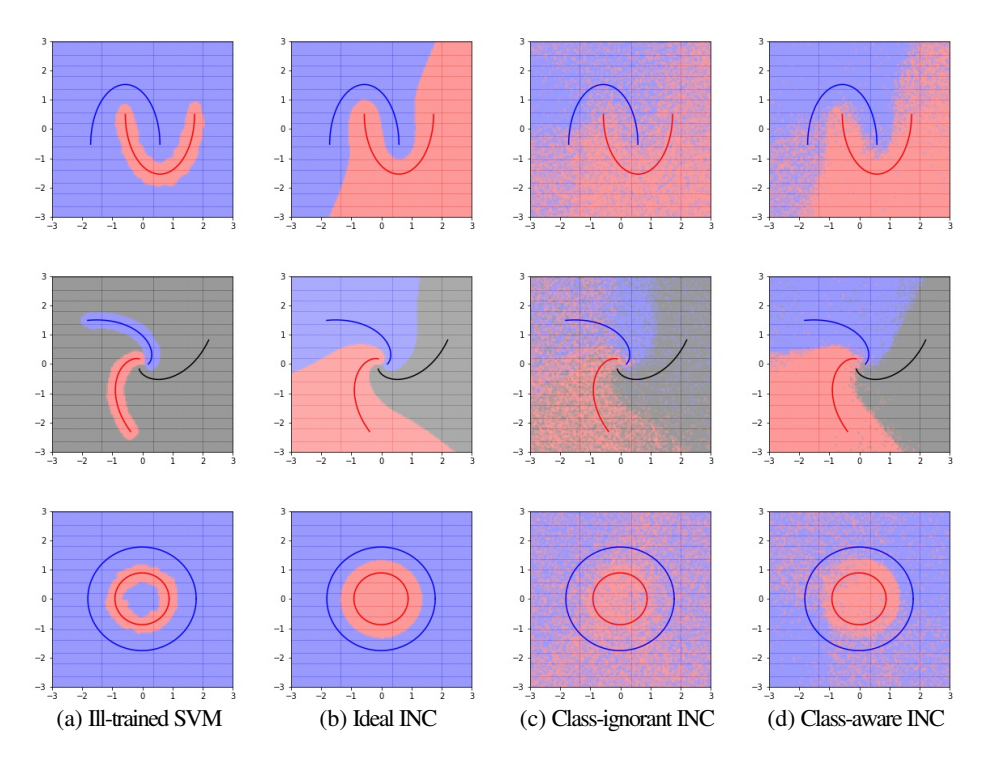


Figure 6: Changes in the decision boundaries of ill-trained SVM after INC applications.

Figure 7 presents the histogram of the projection errors distributed from 0 to the diameter of the distribution. Each row corresponds to each dataset, whereas the first column and the second column represent the results from the class-ignorant model and the class-aware model, respectively. All histograms are normalized so that the sum of values add upto 1. To explain, the y-axis of each histogram is the estimated probability that INC achieves the projection error on the x-axis. Not only that we can observe the improved mean of projection errors in the histograms, but we can also check the reduced standard deviation, i.e. we get more consistent projection errors near the mean.

6 CONCLUSION

In this project, we theoretically and experimentally discussed the necessity of topology-awareness in the training of generative models, especially in security-critical application.

Based on the manifold assumption, we first presented a model of data generation based on the manifold assumption. Then, we explored the theoretical condition when the λ -density level set topologically conforms to the data generating manifold. Theoretically, a continuous generative model should reflect the topological mismatch between the λ -density level sets of the latent vector distribution and of the target distribution. Such mismatch suggests potential problems of defense strategies (against adversarially perturbed examples) exploiting generative models.

We experimentally verified that topology-aware training can prevent the problems from mismatch, thereby improving the performance of any application of generative models. Specifically, we described two different cases of INC optimization failure: the bad initialization and the artifacts induced by the topological difference. After training the generative model with latent vector distribution conforming the number of connected components, the projection error of INC fell down to 30% of the error of INC without topology-aware training.

REFERENCES

Anish Athalye, Nicholas Carlini, and David Wagner. Obfuscated gradients give a false sense of security: Circumventing defenses to adversarial examples. *arXiv preprint arXiv:1802.00420*, 2018.

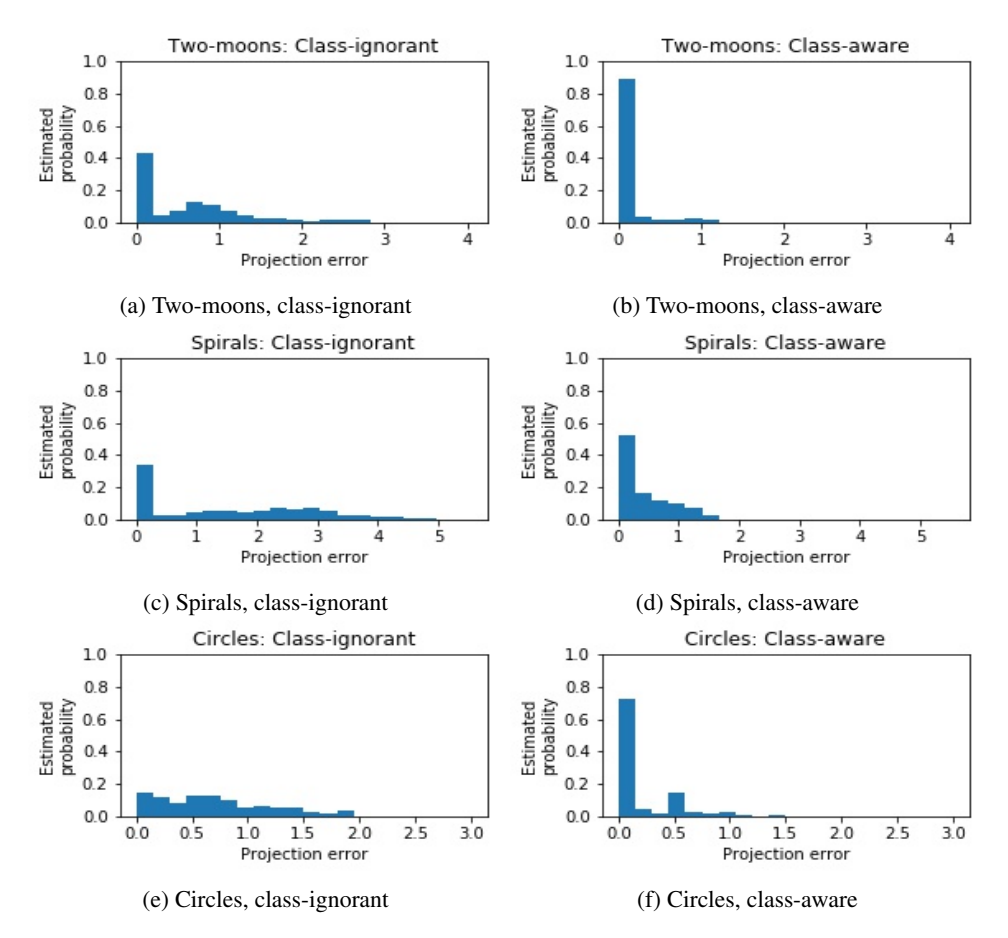


Figure 7: Histograms of the projection errors of INC. Each y-axis represents the estimated probability that INC incurs the projection error on the corresponding x-axis.

Laurent Dinh, Jascha Sohl-Dickstein, and Samy Bengio. Density estimation using real nvp. *arXiv* preprint arXiv:1605.08803, 2016.

Abhimanyu Dubey, Laurens van der Maaten, Zeki Yalniz, Yixuan Li, and Dhruv Mahajan. Defense against adversarial images using web-scale nearest-neighbor search. *arXiv preprint arXiv:1903.01612*, 2019.

Reuben Feinman, Ryan R Curtin, Saurabh Shintre, and Andrew B Gardner. Detecting adversarial samples from artifacts. *arXiv preprint arXiv:1703.00410*, 2017.

Ian Goodfellow, Jean Pouget-Abadie, Mehdi Mirza, Bing Xu, David Warde-Farley, Sherjil Ozair, Aaron Courville, and Yoshua Bengio. Generative adversarial nets. In *Advances in neural information processing systems*, pp. 2672–2680, 2014a.

Ian J Goodfellow, Jonathon Shlens, and Christian Szegedy. Explaining and harnessing adversarial examples. *arXiv preprint arXiv:1412.6572*, 2014b.

Will Grathwohl, Ricky TQ Chen, Jesse Betterncourt, Ilya Sutskever, and David Duvenaud. Ffjord: Free-form continuous dynamics for scalable reversible generative models. *arXiv preprint arXiv:1810.01367*, 2018.

Andrew Ilyas, Ajil Jalal, Eirini Asteri, Constantinos Daskalakis, and Alexandros G Dimakis. The robust manifold defense: Adversarial training using generative models. *arXiv preprint arXiv:1712.09196*, 2017.

Heinrich Jiang. Density level set estimation on manifolds with dbscan. In *Proceedings of the 34th International Conference on Machine Learning-Volume 70*, pp. 1684–1693. JMLR. org, 2017.

- Diederik P Kingma and Max Welling. Auto-encoding variational bayes. *arXiv preprint* arXiv:1312.6114, 2013.
- Durk P Kingma and Prafulla Dhariwal. Glow: Generative flow with invertible 1x1 convolutions. In *Advances in Neural Information Processing Systems*, pp. 10215–10224, 2018.
- J.M. Lee. *Introduction to Smooth Manifolds*. Graduate Texts in Mathematics. Springer, 2003. ISBN 9780387954486. URL https://books.google.com/books?id=eqfgZtjQceYC.
- Aleksander Madry, Aleksandar Makelov, Ludwig Schmidt, Dimitris Tsipras, and Adrian Vladu. Towards deep learning models resistant to adversarial attacks. *arXiv preprint arXiv:1706.06083*, 2017.
- Seyed-Mohsen Moosavi-Dezfooli, Alhussein Fawzi, and Pascal Frossard. Deepfool: a simple and accurate method to fool deep neural networks. In *Proceedings of the IEEE conference on computer vision and pattern recognition*, pp. 2574–2582, 2016.
- J.R. Munkres. *Topology*. Featured Titles for Topology Series. Prentice Hall, Incorporated, 2000. ISBN 9780131816299. URL https://books.google.com/books?id=XjoZAQAAIAAJ.
- Andrew Y Ng and Michael I Jordan. On discriminative vs. generative classifiers: A comparison of logistic regression and naive bayes. In *Advances in neural information processing systems*, pp. 841–848, 2002.
- Aaron van den Oord, Nal Kalchbrenner, and Koray Kavukcuoglu. Pixel recurrent neural networks. *arXiv preprint arXiv:1601.06759*, 2016.
- George Papamakarios, Theo Pavlakou, and Iain Murray. Masked autoregressive flow for density estimation. In *Advances in Neural Information Processing Systems*, pp. 2338–2347, 2017.
- Nicolas Papernot, Patrick McDaniel, Somesh Jha, Matt Fredrikson, Z Berkay Celik, and Ananthram Swami. The limitations of deep learning in adversarial settings. In 2016 IEEE European Symposium on Security and Privacy (EuroS&P), pp. 372–387. IEEE, 2016.
- Xavier Pennec. Probabilities and statistics on riemannian manifolds: Basic tools for geometric measurements. In *NSIP*, pp. 194–198. Citeseer, 1999.
- Alec Radford, Luke Metz, and Soumith Chintala. Unsupervised representation learning with deep convolutional generative adversarial networks. *arXiv preprint arXiv:1511.06434*, 2015.
- Danilo Jimenez Rezende and Shakir Mohamed. Variational inference with normalizing flows. *arXiv* preprint arXiv:1505.05770, 2015.
- Pouya Samangouei, Maya Kabkab, and Rama Chellappa. Defense-gan: Protecting classifiers against adversarial attacks using generative models. *arXiv preprint arXiv:1805.06605*, 2018.
- Yang Song, Taesup Kim, Sebastian Nowozin, Stefano Ermon, and Nate Kushman. Pixeldefend: Leveraging generative models to understand and defend against adversarial examples. *arXiv* preprint arXiv:1710.10766, 2017.
- Christian Szegedy, Wojciech Zaremba, Ilya Sutskever, Joan Bruna, Dumitru Erhan, Ian Goodfellow, and Rob Fergus. Intriguing properties of neural networks. *arXiv preprint arXiv:1312.6199*, 2013.
- Thomas Tanay and Lewis Griffin. A boundary tilting persepective on the phenomenon of adversarial examples. *arXiv preprint arXiv:1608.07690*, 2016.
- Pascal Vincent and Yoshua Bengio. Manifold parzen windows. In *Advances in neural information processing systems*, pp. 849–856, 2003.
- Junbo Zhao, Michael Mathieu, and Yann LeCun. Energy-based generative adversarial network. *arXiv* preprint arXiv:1609.03126, 2016.
- Xiaojin Zhu and Andrew B Goldberg. Introduction to semi-supervised learning. *Synthesis lectures on artificial intelligence and machine learning*, 3(1):1–130, 2009.

A MATHEMATICAL BACKGROUD

A.1 GENERAL TOPOLOGY

In this section, we introduce definitions and theorems related to general topology appeared in the paper. For more details, all the definitions and theorems can be found in Munkres Munkres (2000).

Definitions in general topology We first provide the precise definitions of the terms we brought from the general topology.

Definition 9 (Topological space). A *topology* on a set X is a collection \mathcal{T} of subsets of X having the following properties.

- 1. \emptyset and X are in \mathcal{T} .
- 2. The union of the elements of any subcollection of \mathcal{T} is in \mathcal{T} .
- 3. The intersection of the elements of any finite subcollection of \mathcal{T} is in \mathcal{T} .

A set X for which a topology \mathcal{T} has been specified is called a *topological space*.

For example, a collection of all open sets in \mathbb{R}^n is a topology, thus \mathbb{R}^n is a topological space. If a topology can be constructed by taking arbitrary union and finite number of intersections of a smaller collection \mathcal{B} of subsets of X, we call \mathcal{B} is a basis of the topology.

Pick a metric d in \mathbb{R}^n and consider \mathcal{B} a set of all open balls in \mathbb{R}^n using the metric d. The topology of \mathbb{R}^n can be constructed by taking \mathcal{B} as a basis. When this construction is possible, metric d is said to *induce the topology*.

Definition 10 (Metrizable space). If X is a topological space, X is said to be *metrizable* if there exists a metric d on the set X that induces the topology of X. A *metric space* is a metrizable space X together with a specific metric d that gives the topology of X.

Since \mathbb{R}^n is equipped with Euclidean metric that induces its topology, \mathbb{R}^n is metrizable.

Continuity and the extreme value theorem Let X and Y be topological spaces In the field of general topology, a function $f: X \to Y$ is said to be *continuous*, if for any subset V open in Y, its inverse image $f^{-1}(V)$ is open in X. Moreover, if f is a continuous bijection whose inverse is also continuous, f is called a *homeomorphism*. The notion of homeomorphism is important as it always preserves topological property, e.g. connectedness, compactness, etc., and this will be used in the further generalization of Theorem 2.

Here, we only introduce the generalized statement of extreme value theorem.

Theorem 4 (Extreme value theorem). Let $f: X \to Y$ be continuous, where Y is an ordered set. If X is compact, then there exist points $\underline{\mathbf{x}}$ and $\overline{\mathbf{x}}$ in X such that $f(\underline{\mathbf{x}}) \leq f(\overline{\mathbf{x}})$ for every $\mathbf{x} \in X$.

Specifically, if a manifold M is a compact subset in \mathbb{R}^n , we may use X=M and $Y=\mathbb{R}$.

Normal space and Urysohn lemma The Urysohn lemma was used to prove the Corollary 2. We first introduce the notion of normal space.

Definition 11 (Normal space). Let X be a topological space that one-point sets in X are closed. Then, X is *normal* if for each pair A, B of disjoint closed sets of X, there exist disjoint open sets containing A and B, respectively.

Urysohn's lemma is another equivalent condition for a space to be normal.

Theorem 5 (Urysohn lemma). Let X be a normal topological space; let A and B be disjoint closed subset in X. Let [a,b] be a closed interval in the real line. Then there exists a continuous map

$$f: X \longrightarrow [a, b]$$

such that $f(\mathbf{x}) = a$ for every \mathbf{x} in A, and $f(\mathbf{x}) = b$ for every \mathbf{x} in B.

To apply this lemma to \mathbb{R}^n , we only need the following theorem.

Theorem 6. Every metrizable space is normal.

Since \mathbb{R}^n is metrizable, it is a normal space by Theorem 6. Therefore, we can apply Urysohn lemma to any pair of disjoint subsets in \mathbb{R}^n , to show the existence of a continuous map $f: X \to [0,1]$.

A.2 DIFFERENTIAL GEOMETRY

In this section, we provide the definitions from differential geometry Lee (2003) used in the paper.

Manifold and tangent space

Definition 12 (Manifold). Suppose M is a topological space. We say M is a topological manifold of dimension k if it has the following properties.

- 1. For any pair of distinct points $\mathbf{x}_1, \mathbf{x}_2 \in M$, there are disjoint open subsets $U_1, U_2 \subset M$ such that $\mathbf{x}_1 \in U$ and $\mathbf{x}_2 \in V$.
- 2. There exists a countable basis for the topology of M.
- 3. Every point has a neighborhood U that is homeomorphic to an open subset \tilde{U} of \mathbb{R}^k .

There are different ways to define tangent space of k-dimensional manifold M. Informally, it can be understood as *geometric tangent space* to $M \subset \mathbb{R}^n$ at a point $\mathbf{x} \in M$, which is a collection of pairs (\mathbf{x}, \mathbf{v}) where \mathbf{v} is a vector tantgentially passing through \mathbf{x} . Here we put a more formal definition of tengent space. Consider a vector space $C^{\infty}(M)$, a set of smooth functions on M.

Definition 13 (Tangent space). Let x be a point of a smooth manifold M. A linear map $X: C^{\infty}(M) \to \mathbb{R}$ is called a *derivation at* x if it satisfies

$$X(fg) = f(\mathbf{x})Xg + g(\mathbf{x})Xf$$

for all $f, g \in C^{\infty}(M)$.

The set of all derivations of $C^{\infty}(M)$ at \mathbf{x} forms a vector space called the *tangent space* to M at \mathbf{x} , and is denoted by $T_{\mathbf{x}}(M)$.

Riemannian metric As tangent space $T_{\mathbf{x}}(M)$ is a vector space for each $\mathbf{x} \in M$, we can consider a inner product g_{bfx} defined on $T_{\mathbf{x}}(M)$.

Definition 14 (Riemannian metric). A *Riemannian metric* g on a smooth manifold M is a smooth collection of inner products $g_{\mathbf{x}}$ defined for each $T_{\mathbf{x}}(M)$. The condition for smoothness of g is that, for any smooth vector fields \mathcal{X} , \mathcal{Y} on M, the mapping $\mathbf{x} \mapsto g_{\mathbf{x}}(\mathcal{X}|_{\mathbf{x}}, \mathcal{Y}|_{\mathbf{x}})$.

A manifold M equipped with a Riemannian metric g is called a Riemannian manifold.